Rajnish Grewal[1], Sunita Dahiya[2], Sunil Kumar[3], Naveen Kumar[4]*

[1, 2]Department of Physics, Baba Mastnath University Rohtak, Haryana, India, [3]Department of Physics, RR BAWA DAV College, Batala (143505), Punjab, India, [4]Department of Physics, Panjab University Chandigarh, Chandigarh, India

Scientific paper
ISSN 0351-9465, E-ISSN 2466-2585
https://doi.org/10.62638/ZasMat1136

Zastita Materijala 65 (2)
285 - 293 (2024)

Structural, microstructural, magnetic and dielectric properties of Fe_2O_3 modified CuO composite

ABSTRACT

1-xCuO-xFe_2O_3 composites where x = 0.05, 0.10, 0.15 and 0.20 have been synthesized using ball milling mixing method. The structural, microstructural, elemental analysis, magnetic and dielectric properties of prepared ceramic composites have been investigated using the advanced characterization techniques.The influence of sintering tempearture on structural, dielectric and magnetic properties have been investigated. The structral phase analysis has been carried out using X-ray diffraction and effect of sintering tempertaure clearly depicted in graphs. As increase in sintering temperature from 700 °C to 900 °C, diffraction peaks shift towards higher angles, indicating changes in crystal lattice parameters and potential crystal structure distortions. However, after careful consideration of the XRD results and a comprehensive analysis, we concluded that a synthesis temperature of 700 °C is preferable. The SEM micrographs shows an increase in grain size of ceramic composites as concentrtaion of Fe_2O_3 increases. The Energy Dispersive X-Ray spectroscopy affirms presence of elements according to stoichiometric proportion whereas S-shaped M vs. H. loop confirms presence of magnetic ordering. Variation of Real (ε') and Imaginary (ε") parts of dielectric permittivity with frequency shows genernal dielectric behavior.

Keywords: *Composites, Ball milling mixing method, Dielectric properties, Magnetic properties*

1. INTRODUCTION

Semiconducting nano crystalline materials draw attention for their vast usage in micro-electronics industry due to their small band gap. Transition metal oxide (CuO) based semiconductor having small band gap (1.2-1.5 ev) become important candidates for their usage in digital as well as in electronic industry. CuO is unique and important for wide range applications such as including photochemical cells, gas sensors, biosensors, solar cells, and photocatalytic properties. Current research on pure and modified CuO provides significant potential in realm of microelectronics because of its extraordinarily high dielectric constant. It has been reported in literature that synthesis methods impact on particle size as well as on dielectric behavior of CuO. These are so many synthesis methods to synthesize CuO reported in literature such as sol-gel and sono-chemical method, thermal decomposition method and precipitation method [1-8].

According to Zhu et. al.'s investigation into structural characterization of CuO nano-particles created by microwave irradiating copper (II) acetate and sodium hydroxide as starting material. The particles have a regular shape and limited size distribution as well as high degree of purity. Kim et al. investigated structural, optical, and electrical characteristics of CuO nano-particles with a monoclinic structure phase [9]. From x-ray photoelectron spectroscopy profile, O is 1s and Cu 2p peaks corresponding to the CuO nano-particle were seen. The band gap of CuO nano-particle at room temperature was discovered to be 3.63ev [9].

In this paper, we report structural, elemental, magnetic as well as dielectric properties of Fe_2O_3 modified CuO composites ($_{1-x}CuO$-$_xFe_2O_3$ where x=0.05, 0.10, 0.15 & 0.20) synthesized using Ball mixing method. The major aspect of choosing Fe_2O_3 is modification in magnetic and dielectric properties of CuO ceramics.

*Corresponding author: Sunil Kumar
E-mail: sunil_nano@yahoo.com
Paper received: 28. 09. 2023.
Paper accepted: 30. 12. 2023.
Paper is available on the website: www.idk.org.rs/journal

2. EXPERIMENTAL

1-xCuO-$x$$Fe_2O_3$ composites where x = 0.05, 0.10, 0.15 & 0.20 have been successfully synthesized using ball mixing method. For synthesis of composites, CuO & Fe_2O_3 mixed in required stoichiometric proportion. The CuO and Fe_2O_3 purchased from Sigma Aldrich. The weighed powders of oxides (CuO & Fe_2O_3) transferred in a plastic bottle contains zirconia ball and ball milled in high-energy ball milling machine for 12 hours. After 12hours, mixture of powder and acetone has been taken out from bottle and heated at 100 °C for ~ 1 hour so that acetone get evaporated and powder dried. Dried powder mixed with polyvinyl alcohol (2%wt) as binder and pressed into circular disc (Diameter ~ 12 mm, Thickness ~ 1 mm and Pressure ~ 1.5 ton).

The pallets have been sintered at 700° & 900°C for 2 hours for optimization of sintering temperature at which sample exhibits enhanced magnetic and dielectric properties. The presence of both phases (Structural Phase of CuO & Fe_2O_3) confirmed from X-Ray diffractograms whereas morphological analysis (Grain Growth as well as Grain Size) studied from SEM micrographs. The presence of elements as per stoichiometric proportion mentioned above confirmed using Energy Dispersive X-ray Dispersive spectroscopy whereas elemental mapping shows uniform distribution of different-different metal ions. The density of sintered pellet was measured using lab made set up based on Archimedes principle. The magnetic ordering has been confirmed using Vibrating Sample Magnetometer. The ε', ε" & σ_{ac} vs. Frequency measurements were carried out using impedance analyser.

3. RESULTS AND DISCUSSION

Room temperature structural phase formation has been studied using x-ray diffractograms of CuO, Fe_2O_3 & 1-xCuO-$x$$Fe_2O_3$ composites where x = 0.05, 0.10, 0.15 & 0.20 sintered at 700°C and 900°C shown in figure 1. Sharp high intensity diffraction peaks reveal crystalline nature of prepared ceramic composites whereas noise in background data of Fe_2O_3 results due to fluorescence effect. The diffraction data (diffraction peaks) have been matched with reported JCPDS cards which gives crystallographic information of structural phase of CuO and Fe_2O_3.

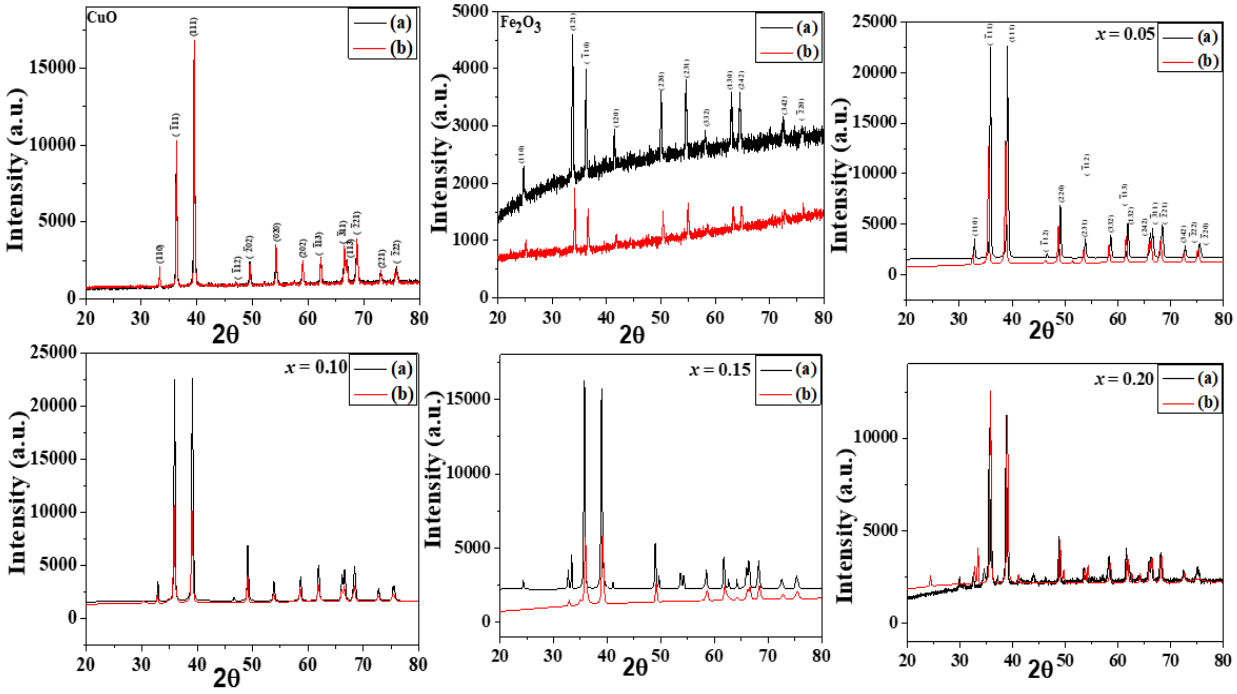

Figure 1. X-Ray Diffraction data of 1-xCuO-xFe_2O_3 where (a) = Sintered at 700°C & (b) 900°C for CuO, Fe_2O_3 and x = x = 0.05, 0.10, 0.15 & 0.20 ceramic composites

Slika 1. Podaci difrakcije rendgenskih zraka 1-xCuO-xFe_2O_3 gde je (a) = sinterovano na 700°C & (b) 900°C za CuO, Fe_2O_3 i x = x = 0,05, 0,10, 0,15 i 0,20 keramičkih kompozita

The experimental data has been indexed according to JCPDS card no 80-1917 (ICDS # 069750) represent for Monoclinic phase space group Cc No. 9 for pure CuO and no. 73-2234 (ICDS # 024791) reports Hexagonal phase space group R $\bar{3}$c for Fe_2O_3. No diffraction peak left unassigned shows that CuO and Fe_2O_3 exhibits its own phase reported in literature. In graphs, for x = 0.05 & 0.10, diffraction peaks quiet well overlapped at both temperatures shows that sample exhibits similar phases but as 'x' increases up to x = 0.15 to 0.20, diffraction peaks shift towards higher 2θ shows change in structural phase with sintering temperature and maximum in x = 0.20. This change in structural phase may result due to strain produced with increasing sintering temperature or increasing concentration of Fe_2O_3 in ceramic composites. Therefore it has been concluded that sample sintered at 700 °C demonstrtaed structural phase of CuO (Monoclinic Phase).

The microstructural analysis of CuO, Fe_2O_3 & 1-xCuO-$x$$Fe_2O_3$ composites where x = 0.05, 0.10, 0.15 & 0.20 sintered at 700°C has been studied from FESEM micrographs and shown in figure 2. Micrographs clearly expresses presence grains with irregular in shape, size and randomly orientated with proper grain growth. All the micrographs were recorded using in-lens detector at 20k magnification & 10 kV accelerating voltage. The increase in grain size with increasing 'x' shows increase in grain growth with least porosity. The grain size has been calculated using Smart SEM software equipped with FESEM. The grain size increases from ~1.46 μm to ~2.26 μm as 'x' increases from 0.05 to 0.20. The density has also been increased from from 6.98 to 7.38 g/cm^3, respectively as 'x' increases.

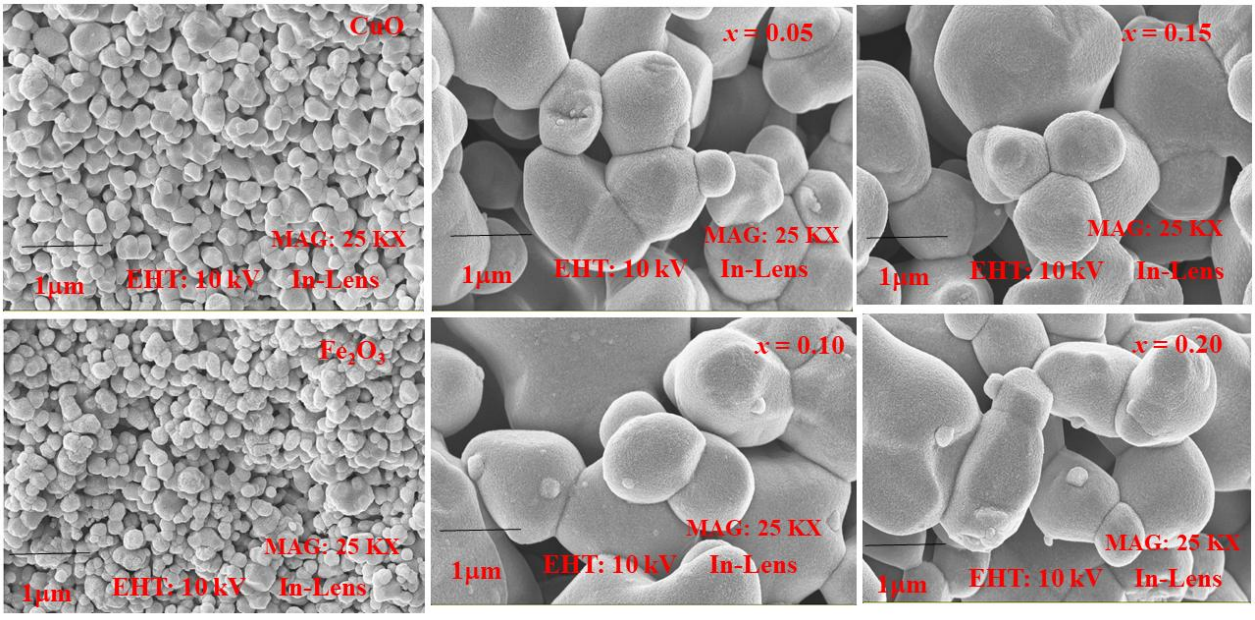

Figure 2. FESEM Micrographs of CuO, Fe_2O_3 and 1-xCuO-xFe_2O_3 where x = x = 0.05, 0.10, 0.15 & 0.20 ceramic composites

Slika 2. FESEM Mikrogrami CuO, Fe_2O_3 i 1-xCuO-xFe_2O_3 gde je x = x = 0.05, 0.10, 0.15 i 0.20 keramičkih kompozita

The presence of elements as per stoichiometric formula have been confirmed from Energy Dispersive X-ray spectroscopy (EDS) analysis. The EDS spectra of pure CuO, Fe_2O_3 and 0.8CuO-0.2Fe_2O_3 ceramic composite sintered at 700 °C have been shown in Figure 3. The Binding Energy vs. Intensity electro micrographs shows that peak corresponding to 8.04 eV, 0.542 & 6.39 eV of Kα evident for presence Cu & O in CuO and Fe and O in Fe_2O_3. The presence of Cu, O & Fe in wt% as well as in mol% has been shown in Table shown in figure 4.

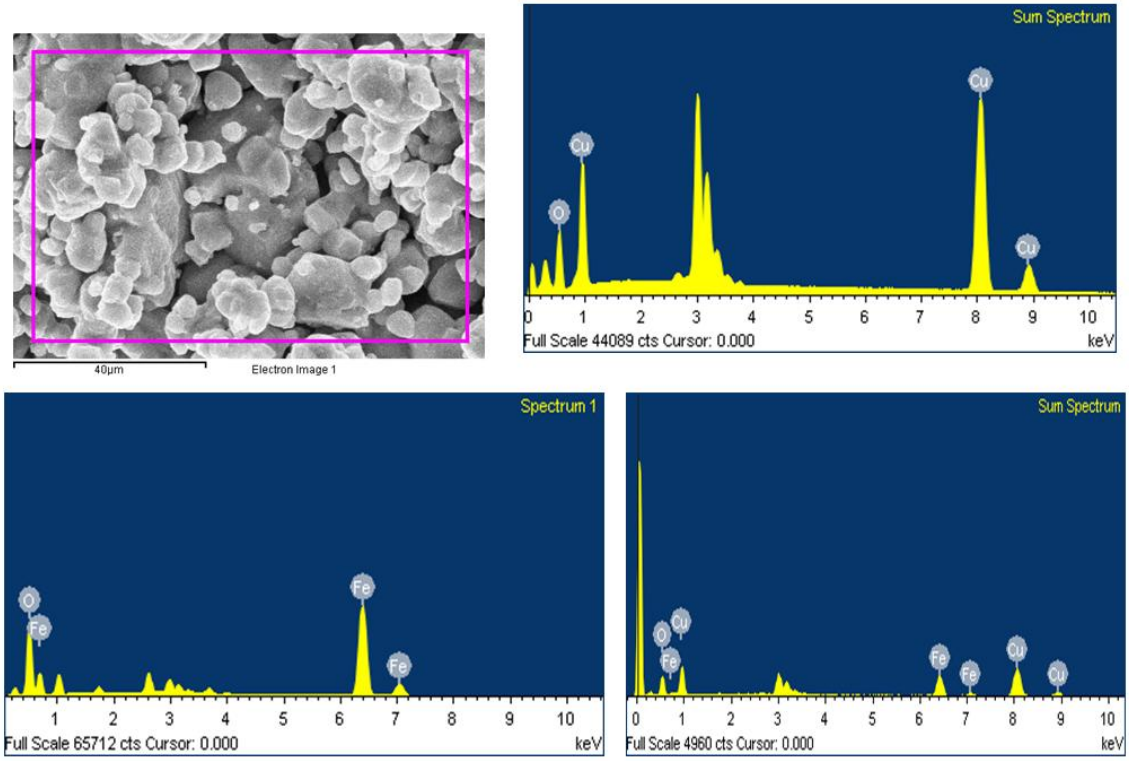

Figure 3. Energy Dispersive Spectral Micro Graphs of CuO, Fe_2O_3 and 0.8CuO-0.2Fe_2O_3 ceramic composites sintered at 700°C

Slika 3. Energetski disperzivni spektralni mikrografovi CuO, Fe_2O_3 i 0.8CuO-0.2Fe_2O_3 keramičkih kompozita sinterovanih na 700°C

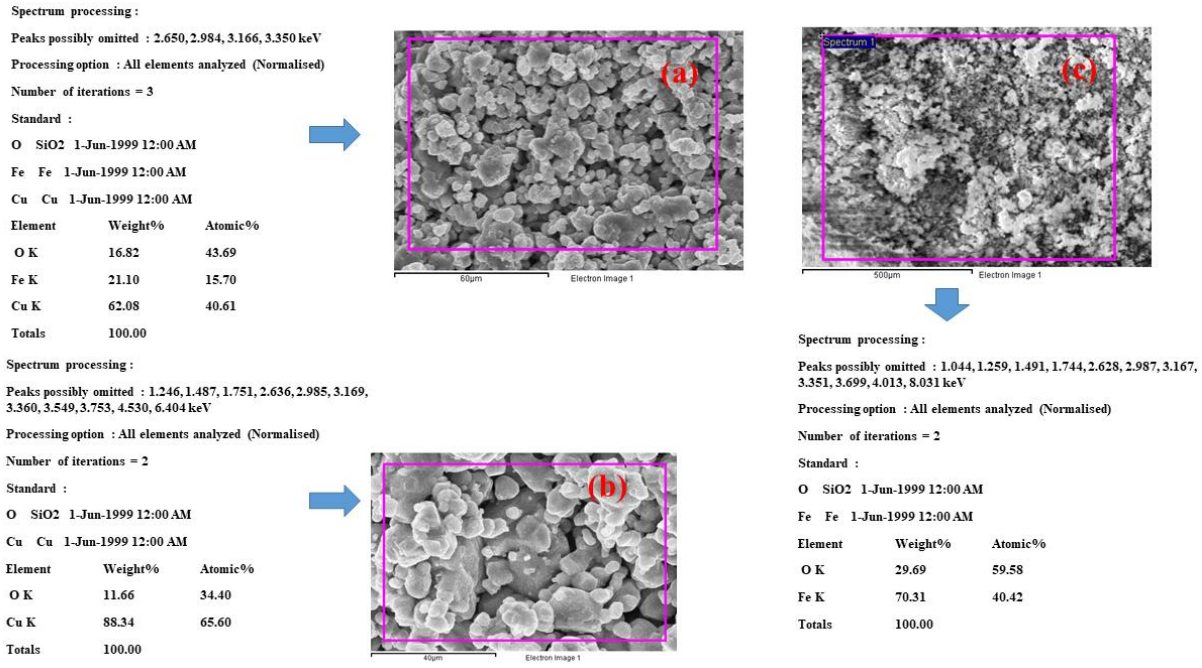

Figure 4. Weight (%) and Mol (%) of CuO, Fe_2O_3 and 0.8CuO-0.2Fe_2O_3 ceramic composites sintered at 700°C

Slika 4. Težina (%) i mol (%) CuO, Fe_2O_3 i 0.8CuO-0,2Fe_2O_3 keramičkih kompozita sinterovanih na 700°C

The distribution of different metal ions as per stoichiometric formula, Elemental mapping in selected area has been carried out. The elemental mapped electron micrographs of CuO, Fe_2O_3 & $0.8CuO\text{-}0.2Fe_2O_3$ ceramic composites sintered at 700 °C shown in figure 5. The different colours have been assigned to different metal ions. The micro-graphs with all coloured dot show that all metal ions distributed uniformly. The red colour assigned to Cooper (Cu) whereas Oxygen (O) and Iron (Fe) green and yellow colour. The micrograph in which all colour represents uniformly presence of all metal ions in selected area.

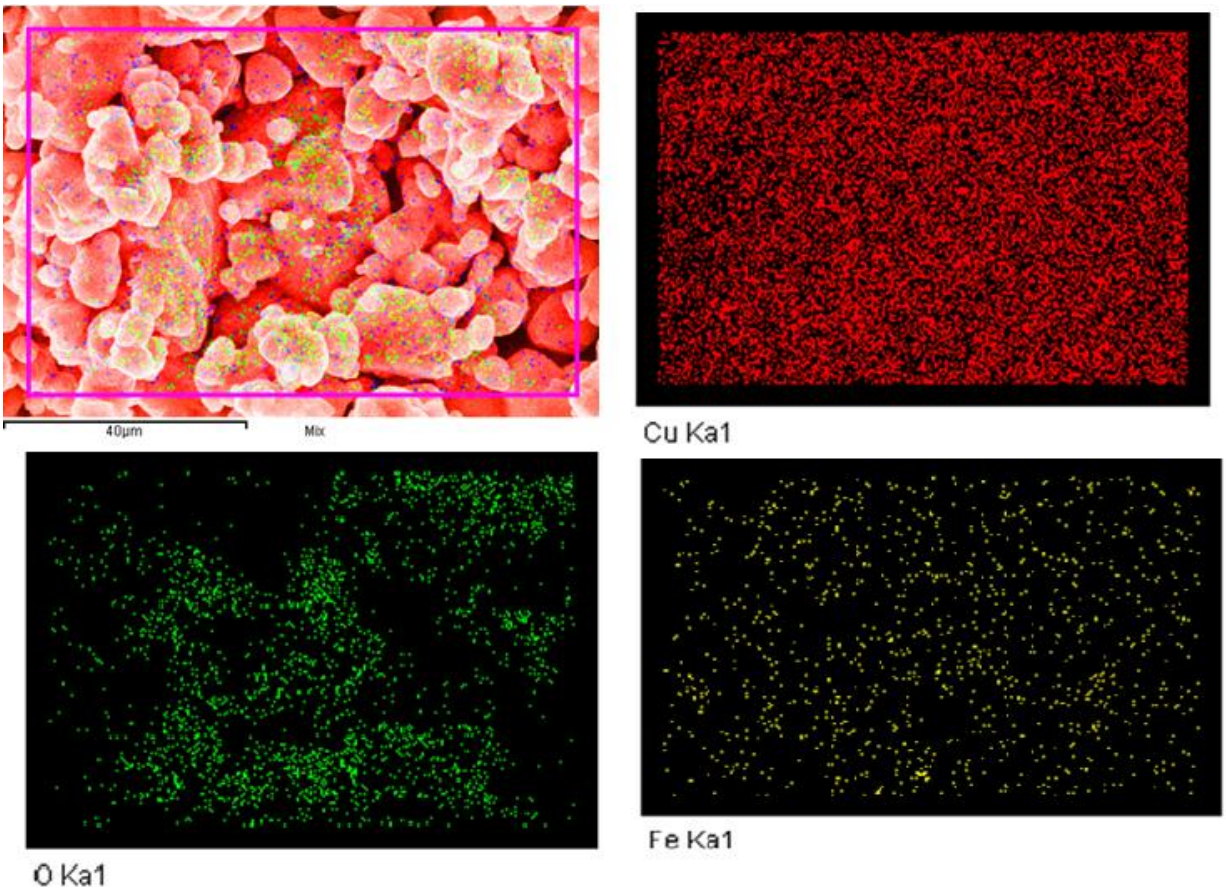

Figure 5. Elemental Mapping along with mixed micrograph of $0.8CuO\text{-}0.20Fe_2O_3$ ceramic composites sintered at 700°C

Slika 5. Elementarno mapiranje zajedno sa mešovitim mikrografijom $0.8CuO\text{-}0.20Fe_2O_3$ keramičkih kompozita sinterovanih na 700°C

Magnetization vs. Magnetic Field measure-ments of CuO, Fe_2O_3 & $1\text{-}xCuO\text{-}xFe_2O_3$ composites where x = 0.05, 0.10, 0.15 & 0.20, sintered at 700°C have been shown in figure 6. The magnetic data clearly reveal that (a) Small remnant magnetization value and narrow coercivity of CuO results for superparamagnetic or week magnetic ordering as already reported (b) magnetic hysteresis of Fe_2O_3 sintered at 700 °C magnetically ordered behavior. The hysteresis in $1\text{-}xCuO\text{-}xFe_2O_3$ samples sintered at 700 °C reveals dominance of ferromagnetic ordering over antiferromagnetic (Presence of Both Ferromagnetic as well as antiferromagnetic confirmed from unsaturated hysteresis curve). Such kind of behavior (Presence of both Ferromagnetic and Antiferromagnetic ordering) may be due to oxygen vacancies created which results in pinched hysteresis loop. The remnant magnetization (M_r) of prepared ceramic composites increases from 0.068 emu/g for x = 0.05 to 0.118 emu/g for x = 0.15 and then decreases to 0.099 emu/g for x = 0.20 whereas coercivity also varies from 393.8 Oe for x = 0.05 to 438.6 Oe for x = 0.15 and then decreases to 296.2 Oe for x = 0.20. Since CuO is exhibits weakly magnetic or superparamagnetic behavior. This increase in remnant magnetization may result due to increase in creation of oxygen, which create multi valance state of Fe (Fe^{2+} & Fe^{3+}) during sintering in oxygen deficient environment. These

oxygen vacancies responsible for strong negative super exchange interaction between Fe^{3+} and Fe^{3+} through oxygen (O^{2-}) anion responsible for antiferromagnetic ordering whereas direct exchange interaction between Fe^{3+}/Fe^{3+} and Fe^{3+}/Fe^{2+} through vacancies (V_o) results in ferromagnetic ordering. The increase in value of M_r may be due to increased effect of Fe^{3+}/Fe^{3+} and Fe^{3+}/Fe^{2+} through vacancies (V_o) which results in ferromagnetic ordering [10]. The value of remnant magnetization (emu/g) and coercivity (Oe) tabulated in Table 1. It is clear that direct exchange interaction between Fe^{3+}/Fe^{3+} and Fe^{3+}/Fe^{2+} through vacancies (V_o) dominates over strong negative super exchange interaction between Fe^{3+} and Fe^{3+} through oxygen (O^{2-}) anion up to x = 0.15 and then reverses responsible for increase in remnant magnetization up to x = 0.15 and then decreases.

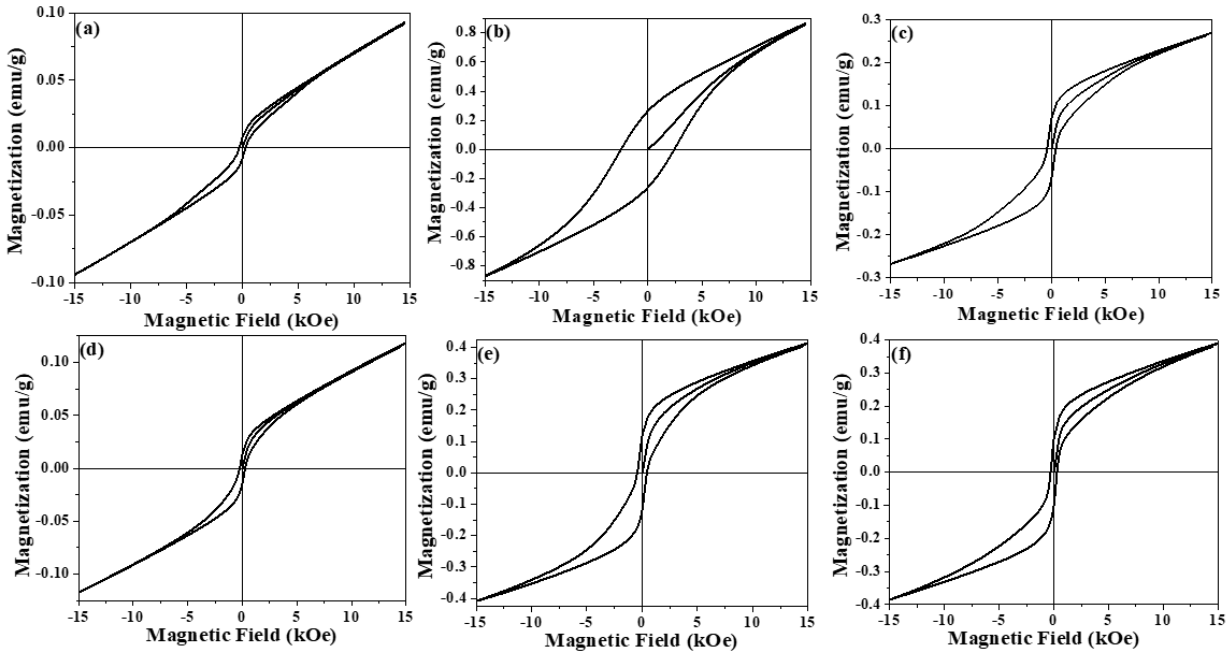

Figure 6. Magnetization vs. Applied Magnetic Field of CuO, Fe_2O_3 & 1-xCuO-xFe_2O_3 where (a) = CuO, (b) = Fe_2O_3(c) = 0.05, (d) = 0.10, (e) = 0.15 & (f) = 0.20 ceramic composites sintered at 700 °C

Slika 6. Magnetizacija u odnosu na primenjeno magnetno polje CuO, Fe_2O_3 i 1-CuP-Fe_2O_3 gde je (a) = CuP, (b) = Fe_2O_3(c) = 0.05, (d) = 0.10, (e) = 0.15 & (f) = 0.20 keramičkih kompozita sinterovanih na 700°C

Table 1. The Value of Remnant Magnetization & Coercive Field of CuO, Fe_2O_3 & 1-xCuO-xFe_2O_3 where (a) = CuO, (b) = Fe_2O_3(c) = 0.05, (d) = 0.10, (e) = 0.15 & (f) = 0.20 ceramic composites sintered at 700°C

Tabela 1. Vrednost preostale magnetizacije i koercitivnog polja CuO, Fe_2O_3 i 1-kCuO-kFe_2O_3 gde je (a) = CuO, (b) = Fe_2O_3(c) = 0.05, (d) = 0.10, (e) = 0.15 & (f) = 0.20 keramičkih kompozita sinterovanih na 700°C

Sample	M_r (emu/g)	H_c (Oe)
(a)	0.007	276.6
(b)	0.262	2461
(c)	0.068	393.8
(d)	0.013	254.9
(e)	0.118	438.6
(f)	0.099	296.2

Room temperature variation of Real & Imaginary part of dielectric permittivity (ε') & (ε") of CuO & 1-xCuO-xFe_2O_3 composites where x = 0.05, 0.10, 0.15 & 0.20 in frequency range varies from 100Hz -1MHz have been shown in figure 7 & 8. It has been clearly revealed from graphs that value of both Real (ε') and Imaginary (ε") part of dielectric permittivity decreases as frequency increases up to a certain value and afterward varies linear. In lower frequency range, both Real & Imaginary part of dielectric permittivity (ε') & (ε") exhibits maximum value and decreases continuously with increasing frequency and become almost linear after certain value of frequency. Such types of behavior of represent general dielectric behavior of any dielectric, which follow either Debye, or Non-Debye behavior. In lower frequency range, maximum of all polarizations (Dipolar, Ionic, Electronic &

Interfacial) effectively contributes to dielectric permittivity results in maximum value of both Real (ε') and Imaginary (ε") part of dielectric permittivity [11,12].

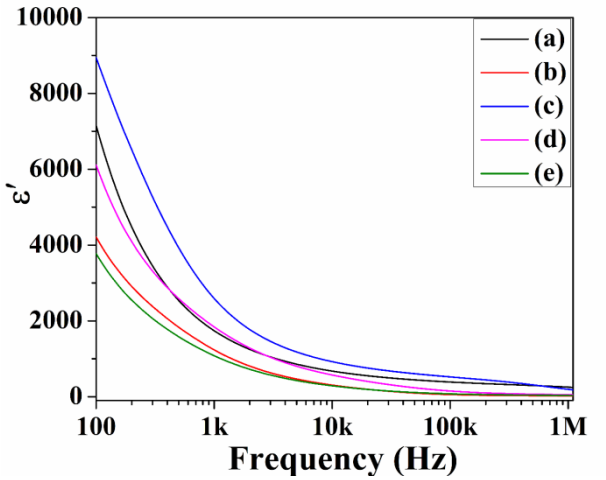

Figure 7. ε' vs. Frequency of CuO, Fe_2O_3 & 1-xCuO-xFe_2O_3 where (a) = CuO, (b) = Fe_2O_3 (c) = 0.05, (d) = 0.10, (e) = 0.15 & (f) = 0.20 ceramic composites sintered at 700°C

Slika 7. ε' u odnosu na učestalost CuO, Fe_2O_3 i 1-xCuO-xFe_2O_3 gde je (a) = CuO, (b) = Fe_2O_3 (c) = 0.05, (d) = 0.10, (e) = 0.15 & (f) = 0.20 keramički kompoziti sinterovani na 700°C

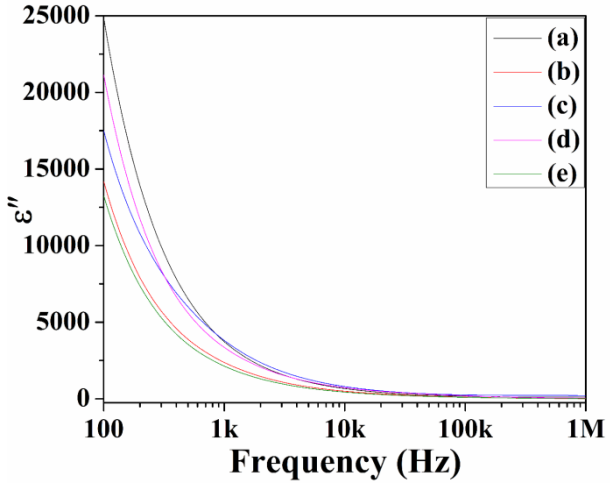

Figure 8. ε" vs. Frequency of CuO, Fe_2O_3 & 1-xCuO-xFe_2O_3 where (a) = CuO, (b) = Fe_2O_3 (c) = 0.05, (d) = 0.10, (e) = 0.15 & (f) = 0.20 ceramic composites sintered at 700 °C

Slika 8. ε" naspram učestalosti CuO, Fe_2O_3 i 1-xCuO-xFe_2O_3 gde je (a) = CuO, (b) = Fe_2O_3 (c) = 0.05, (d) = 0.10, (e) = 0.15 & (f) = 0.20 keramički kompoziti sinterovani na 700°C

As frequency increases towards higher regime, value of both Real (ε') and Imaginary (ε") part of dielectric permittivity starts decreases and after certain value of frequency, value of both Real (ε') and Imaginary (ε") part of dielectric permittivity become almost constant. This may be due to elimination of contribution of polarization in dielectric permittivity. It has been clearly seen from graph that value dielectric permittivity first decreases and then increases up to maximum value as '*x*' increases and again decreases with further increase of '*x*' may be due to interfacial polarization.

The Cole-Cole relaxation model (modified form of Debye relaxation model) has been used to explain the relaxation phenomenon [12]. According to this model, the ε′ and ε″ vary with frequency as:

$$\varepsilon'(\omega) = \varepsilon_\infty + (\varepsilon_s - \varepsilon_\infty)\frac{1 + (\omega\tau_0)^{1-\alpha}\sin\frac{1}{2}\alpha\pi}{1 + 2(\omega\tau_0)^{1-\alpha}\sin\frac{1}{2}\alpha\pi + (\omega\tau_0)^{2(1-\alpha)}}$$

$$\varepsilon''(\omega) = (\varepsilon_s - \varepsilon_\infty)\frac{(\omega\tau_0)^{1-\alpha}\cos\frac{1}{2}\alpha\pi}{1 + 2(\omega\tau_0)^{1-\alpha}\sin\frac{1}{2}\alpha\pi + (\omega\tau_0)^{2(1-\alpha)}}$$

Where ε_∞ = dielectric constant measured at high frequency, ε_s = dielectric constant measured at low frequency, ω = 2πf the angular frequency of applied field and τ = characteristics relaxation time of the medium. The exponent parameter α usually varies between 0 and 1, and it describes shape of spectral curves. It may be noted that for α =0, Cole-Cole model reduces to Debye model.

Room temperature σ_{ac} vs. Frequency at room temperature CuO, Fe_2O_3 & 1-*x*CuO-*x*Fe_2O_3 composites where *x* = 0.05, 0.10, 0.15 & 0.20, sintered at 700°C have been shown in figure 8. The ac conductivity calculated from recorded dielectric parameters using following formula

$$\sigma_{ac} = 2\pi f \varepsilon' \varepsilon_o \tan\delta$$

Where the parameters have their usual meaning. Ac conductivity profile with frequency has been divided into two regions. First linearly varied region with frequency known as dc conductivity whereas dispersion region which corresponds to ac conductivity. Frequency varied ac conductivity in ceramics is generally analyzed by Jonscher's power law;

$$\sigma_{ac} = \sigma_{dc} + A\,\omega^n,$$

Where "A" is dispersion parameter representing the strength of polarizibilty and "n" dimensionless frequency exponent representing interaction between mobile ions with lattice around them.

According to Jonscher, origin of frequency dependence of conductivity may be due to relaxation phenomenon arising due to hoping of mobile charge carriers [13-16]. The conductivity also follows similar behavior like dielectric behavior. This may also due to variation in concentration of oxygen vacancies created which also effect magnetic properties means remnant magnetization first decreases and then increases may result due to processing of Fe_2O_3 with CuO in CuO-Fe2O3 composites as shown in figure 9.

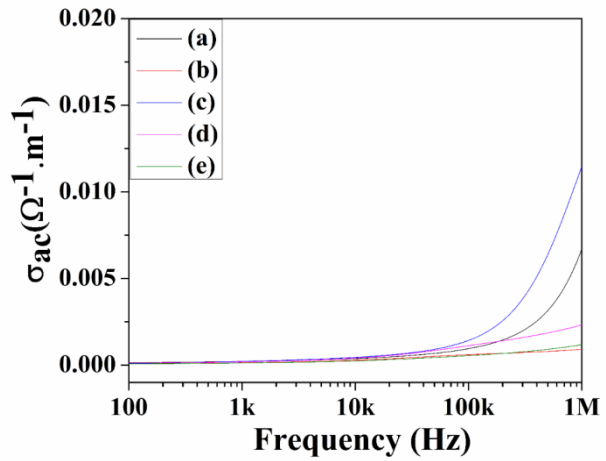

Figure 9. σac vs. Frequency variation of CuO, Fe_2O_3 & 1-xCuO-xFe_2O_3 where (a) = CuO, (b) = Fe_2O_3, (c) = 0.05, (d) = 0.10, (e) = 0.15 & (f) = 0.20 ceramic composites sintered at 700°C

Slika 9. σac naspram varijacije frekvencije CuO, Fe_2O_3 i 1-xCuO-xFe_2O_3 gde je (a) = CuO, (b) = Fe_2O_3 (c) = 0.05, (d) = 0.10, (e) = 0.15 i (f) = 0.20 keramički kompoziti sinterovani na 700°C

4. CONCLUSION

CuO, Fe_2O_3 and 1-*x*CuO-*x*Fe_2O_3 where *x* = 0.05, 0.10, 0.15 & 0.20 ceramic composites sintered at 700 °C & 900 °C where *x* = 0.05, 0.10, 0.15 & 0.20 have been successfully prepared using ball milling mixing method. X-ray diffraction pattern confirms that optimized sintering temperature for ceramic composites is 700 °C at which composites exhibits crystalline phase of both CuO and Fe_2O_3 as reported in JCPDS cards. Microstructural analysis gives densification as well as grain growth whereas energy dispersive x-ray spectroscopy and elemental mapping reveals presence of elements according to mentioned stoichiometric proportion and uniform distribution of metal ions.

Magnetic hysteresis data confirms that variation in magnetization directly follows competition of AFM and FM interaction whereas dielectric data follow similar behavior to magnetic ordering which results from creation of oxygen vacancies. The oxygen vacancies also play an important role in conduction behavior of dielectrics whereas interfacial polarization also plays effective role in dielectric properties of composites.

5. REFERENCES

[1] M.Fterich, F.B.Nasr, R.Lefi, M.Toumi, S.Guermazi (2016) Effect of concentration of hexamethylenetetramine in structure, microstructure and optical properties of CuO nanoparticles synthesized by hydrothermal route. Materials Science in Semiconductor Processing, 43, 114-122. https://doi.org/10.1016/j.mssp.2015.11.023

[2] S.Heikal, H.M.Mokhtar, W.A.E.Ghany (2023) Effect of CuO addition on the structural, electrical and dielectric properties of the sodium borate glasses. Physica B: Condensed Matter, 667, 415142.https://doi.org/10.1016/j.physb.2023.415142

[3] C.Oruç, A.Altındal (2017) Structural and dielectric properties of CuO nanoparticles. Ceramics international, 43(14), 10708-10714. https://doi.org/10.1016/j.ceramint.2017.05.006

[4] M.E.Grigore, E.R.Biscu, A.M.Holban, M.C.Gestal, A.M.Grumezescu (2016) Methods of synthesis, properties and biomedical applications of CuO nanoparticles. Pharmaceuticals, 9(4), 75-83. https://doi.org/10.3390/ph9040075

[5] K.S.Siddiqi, A.Husen (2020) Current status of plant metabolite-based fabrication of copper/copper oxide nanoparticles and their applications: a review. Biomaterials Research, 24(1), 1-15. https://doi.org/10.1186/s40824-020-00188-1

[6] W.Hao, P.Xu, L.Sun, E.Cao (2023) Influence of CuO addition on the sintering temperature and giant dielectric properties of $(In_{0.5}Nb_{0.5})_{0.05}Ti_{0.95}O_2$ ceramics. Ceramics International, 49(24), 40650-40658. http://dx.doi.org/10.1016/j.ceramint.2023.10.046

[7] E.Arulkumar, S.S.Shree, S.Thanikaikarasan (2023) Structure, morphology, composition, optical properties of CuO/NiO nanocomposite for electrochemical energy storage devices. Results in Chemistry, 6, 101087. http://dx.doi.org/10.1016/j.rechem.2023.101087

[8] O.I.Sallam, M.M. Atta, E.O.Taha, A.M.Elbasiony, A. M.A.Henaish, R.M.Ahmed (2023) Synthesis and modification of photoluminescence and dielectric properties of novel fluorophosphate glass by incorporating different transition metal oxides for optoelectronic application. Optical Materials, 136, 113413. https://ui.adsabs.harvard.edu/link_gateway/2023OptMa.13613413S/doi:10.1016/j.optmat.2022.113413

[9] M.E.Grigore, E.R.Biscu, A.M.Holban, M.C.Gestal, A. M. Grumezescu (2016) Methods of synthesis, properties and biomedical applications of CuO nanoparticles. Pharmaceuticals, 9(4), 75-84. https://doi.org/10.3390/ph9040075

[10] K.S.Siddiqi, A.Husen (2020) Current status of plant metabolite-based fabrication of copper/copper oxide

nanoparticles and their applications: a review. Biomaterials Research, 24(1),1-15.
https://doi.org/10.1186/s40824-020-00188-1

[11] S.Kumar, J.Pal, S.Kaur, R.Kaur, M.Singh, A.Singh (2018) The Effect of Aliovalent Pb^{2+} Dopant on the Magnetic and Magnetodielectric Properties of $LaFeO_3$ Solid Solutions. Journal of Magnetism and Magnetic Materials, 467, 89-95.
https://doi.org/10.1016/j.jmmm.2018.07.037

[12] M.Kumar, K.L.Yadav (2007) Study of dielectric, magnetic, ferroelectric and magnetoelectric properties in the $PbMn_xTi_{1-x}O_3$ system at room temperature. Journal of Physics: Condensed Matter, 19, 242202.
https://doi.org/10.1088/0953-8984/19/24/242202

[13] K.S.Cole, H.Robert (1941) Dispersion and Absorption in Dielectrics:-Alternating Current Characteristics. Journal of Chemical Physics, 9, 341–351. http://dx.doi.org/10.1063/1.1750906

[14] S.Havriliak, S.Negami (1967) A complex plane representation of dielectric and mechanical relaxation processes in some polymers. Polymer, 3861(67), 90021-3.
https://doi.org/10.1016/0032-3861(67)90021-3

[15] V.Prakasha, S.N.Choudharya, T.P.Sinhab (2008) Dielectric relaxation in complex perovskite oxide $BaCo_{1/2}W_{1/2}O_3$. Physica B, 403, 103-108.
http://dx.doi.org/10.1016/j.physb.2007.08.015

[16] A.K.Jonscher (1977) The Universal Dielectric Response. Nature, 267, 673-679.
https://ui.adsabs.harvard.edu/link_gateway/1977Natur.267..673J/doi:10.1038/267673a0

IZVOD

STRUKTURNA, MIKROSTRUKTURNA, MAGNETNA I DIELEKTRIČNA SVOJSTVA CuO KOMPOZITA MODIFIKOVANOG Fe_2O_3

1-xCuO-xFe2O3 kompoziti, gde je x = 0,05, 0,10, 0,15 i 0,20, su sintetizovani metodom mešanja sa kugličnim mlevenjem. Pripremljena keramika je okarakterisana po različitim osobinama kao što su strukturna i mikrostrukturna, elementarni sastav prema navedenoj stehiometrijskoj proporciji i magnetna svojstva. Takođe, istraživana su dielektrična svojstva pripremljenih keramičkih kompozita, sinterovanih na različitim temperaturama, na sobnoj temperaturi. Kako povećavamo temperaturu sinteze sa 700 °C na 900 °C, vrhovi difrakcije se pomeraju ka većim uglovima, što ukazuje na promene u parametrima kristalne rešetke i potencijalne izobličenja kristalne strukture. Ova primećena promena ukazuje na povećanu toplotnu energiju koja utiče na raspored atoma u materijalu. Međutim, nakon pažljivog razmatranja XRD rezultata i sveobuhvatne analize, zaključili smo da je temperatura sinteze od 700°C poželjnija. Na ovoj nižoj temperaturi održava se željena kristalna struktura, minimizirajući rizik od strukturnih promena ili faznih transformacija koje bi mogle uticati na svojstva i performanse materijala. Pored toga, izbor od 700°C obezbeđuje ravnotežu između postizanja željenih karakteristika materijala i izbegavanja potencijalnih nedostataka povezanih sa višim temperaturama sinteze. SEM mikrografije pokazuju povećanje veličine zrna keramičkih kompozita. Energetska disperzivna rendgenska spektroskopija potvrđuje prisustvo elemenata u skladu sa stehiometrijskom proporcijom, dok S-oblika M protiv H. petlje potvrđuje prisustvo magnetnog uređenja. Realni (e') i imaginarni (e") delovi dielektrične permitivnosti u odnosu na frekvenciju pokazuju dielektrično ponašanje.

Ključne reči: *Kompoziti, metoda mešanja sa kugličnim mlevenjem, dielektrična svojstva, magnetna svojstva*

Naučni rad
Rad primljen: 28.09.2023.
Rad prihvacen: 30.12.2023.
Rad je dostupan na sajtu: www.idk.org.rs/casopis